Simulated resilience of tropical rainforests to CO$_2$-induced climate change

Chris Huntingford[1]*, Przemyslaw Zelazowski[2], David Galbraith[2,3], Lina M. Mercado[1,4], Stephen Sitch[3,4], Rosie Fisher[5], Mark Lomas[6], Anthony P. Walker[6], Chris D. Jones[7], Ben B. B. Booth[7], Yadvinder Malhi[2], Debbie Hemming[7], Gillian Kay[7], Peter Good[7], Simon L. Lewis[3,8], Oliver L. Phillips[3], Owen K. Atkin[9], Jon Lloyd[3,10], Emanuel Gloor[3], Joana Zaragoza-Castells[11], Patrick Meir[9,11], Richard Betts[7], Phil P. Harris[1], Carlos Nobre[12], Jose Marengo[12] and Peter M. Cox[13]

How tropical forest carbon stocks might alter in response to changes in climate and atmospheric composition is uncertain. However, assessing potential future carbon loss from tropical forests is important for evaluating the efficacy of programmes for reducing emissions from deforestation and degradation. Uncertainties are associated with different carbon stock responses in models with different representations of vegetation processes on the one hand[1-3], and differences in projected changes in temperature and precipitation patterns on the other hand[4,5]. Here we present a systematic exploration of these sources of uncertainty, along with uncertainty arising from different emissions scenarios for all three main tropical forest regions: the Americas (that is, Amazonia and Central America), Africa and Asia. Using simulations with 22 climate models and the MOSES–TRIFFID land surface scheme, we find that only in one[5] of the simulations are tropical forests projected to lose biomass by the end of the twenty-first century—and then only for the Americas. When comparing with alternative models of plant physiological processes[1,2], we find that the largest uncertainties are associated with plant physiological responses, and then with future emissions scenarios. Uncertainties from differences in the climate projections are significantly smaller. Despite the considerable uncertainties, we conclude that there is evidence of forest resilience for all three regions.
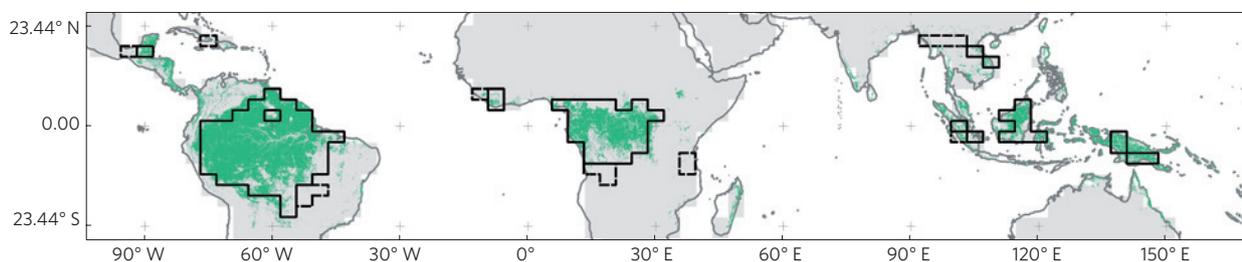
Tropical forests store approximately 470 billion tonnes of carbon in their biomass and soil[6], are responsible for about one-third of global terrestrial primary productivity[7], regulate local meteorology and house a disproportionate amount of global biodiversity[8]. A number of previous analyses have investigated potential vulnerability of tropical forests under climate change (Supplementary Table SA1). Some, based on future projections by the HadCM3 climate model (for example, ref. 5), suggest that anthropogenically induced climate change across Amazonia could cause catastrophic losses of forest cover and biomass (die-back).

This is true when using outputs from that climate model to drive a number of vegetation models[1]. More recently, multiple climate models have been used to force particular vegetation models, hence utilizing an ensemble of climate forcings[4]. In other analyses, alteration of the biogeographical extent of tropical forests is estimated solely by predicting regions that will have meteorological conditions similar to those of the present day and where forest exists (bioclimatic envelope modelling)[9,10]. When forced by general circulation models (GCMs) other than HadCM3, vegetation models have usually simulated lower or even no losses of Amazonian forest cover. There are far fewer assessments of possible climate-change impacts on tropical regions outside Amazonia. Two existing studies[10,11] suggest that significant parts of tropical Africa and Asia may be less sensitive to climate change.

We study projected uncertainty of biomass stocks for the three main tropical forest regions: the Americas (that is, Central America and the Amazonia Basin *sensu lato*), Africa and Asia, and with initial emphasis on a version of the land surface model (MOSES–TRIFFID) similar to ref. 5 (Methods). This is forced with bias-corrected climate-change projections for the tropics based on the 22 climate models used by the Intergovernmental Panel on Climate Change Fourth Assessment. We isolate meteorological drivers and hence the relationship between biomass and changes in temperature[3], precipitation and direct fertilization influence of raised [CO$_2$]. Simulations are compared with recent measurements of tropical forest biomass stocks, by extrapolating forest plot networks[12,13].

Figure 1 shows the geographical distribution of rainforest cover predicted for the initial contemporary state of our land surface model (Methods) forced with Climate Research Unit (CRU) climatology. We find general agreement between the modelled rainforest distribution and the observed distribution. Figure 2 presents simulated terrestrial vegetation carbon content defined as the carbon in above-ground biomass and live roots, C_v (Mg ha^{-1}).

Figure 1 | Map of tropical forest. Shown are tropical land regions and model gridboxes predicted to have more than 85% cover of forest for pre-industrial climate (continuous and dashed black outlines). The green dots are from satellite retrievals of where there is mainly evergreen tropical forest, based on the GLC2000 land cover map. The gridboxes used in our analysis have continuous black outlines. The 15 gridboxes outlined with dashed lines were not included in our analysis as these areas contain little (<10%) observed forest cover, despite the model predicting higher coverage.
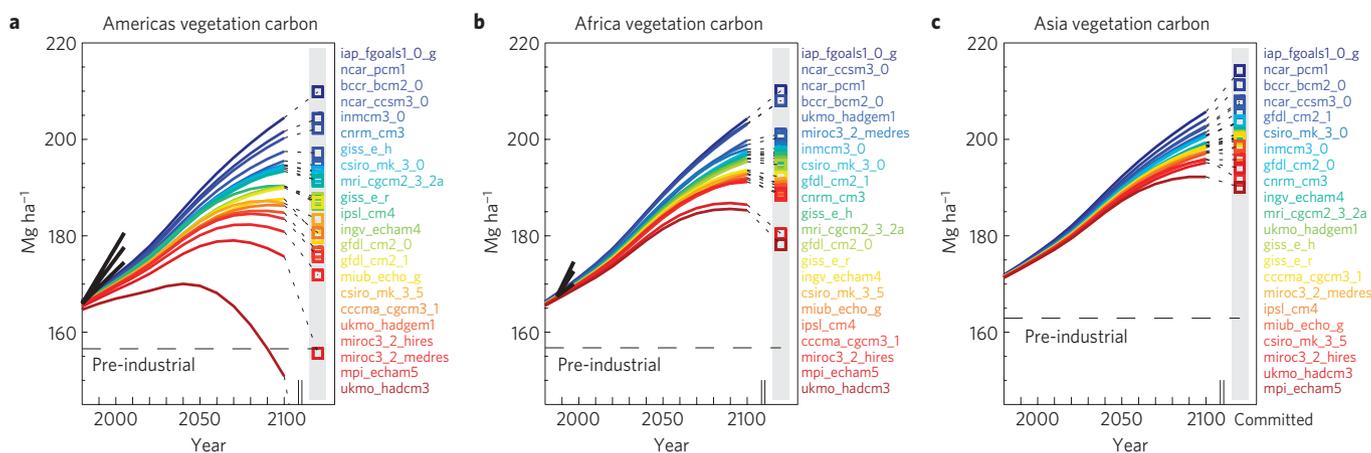

Figure 2 | Biomass change. a–c, Tropical forest biomass predictions for the Americas (**a**), Africa (**b**) and Asia (**c**) by the MOSES–TRIFFID model forced by 22 climate models. Climate models emulated are colour-coded, from dark blue to dark red for decreasing year 2100 values of C_v. Grey regions and squares are committed C_v values with climate constant at year 2100 values, and small dashes link back to the same model in transient predictions. Committed equilibrium values are year-independent, hence the x-axis break (small vertical bars). Normalized estimates of C_v from inventory data (2.5%, mean and 97.5% confidence levels) are the short black curves for Americas and Africa. Horizontal lines (large dashes) are estimated pre-industrial values, year 1860.

This is for the three tropical regions, to year 2100 and driven with atmospheric $[CO_2]$ concentrations and non-CO_2 radiative forcing pathways representative of the Special Report on Emissions Scenarios (SRES) A2 business-as-usual anthropogenic emissions scenario. These predictions have been constructed by emulating the changes in surface meteorology predicted by the 22 climate models, all in the combined climate and land surface impacts system IMOGEN (ref. 14; Methods). Such changes of climate are added to the CRU climatology, taken as representative of pre-industrial conditions and removing significant model biases (Supplementary Fig. S1). For the contemporary period, C_v increases in all simulations and regions, and is compared with normalized forest inventory data (Methods) as the three short black curves for Americas and Africa. The three curves correspond to changes at the 97.5% confidence level, mean change and 2.5% level[12,13]. There is agreement that tropical forests are gaining biomass, although the observational data suggest the increases have been larger than that modelled for the recent period. The magnitude of the increase in tropical forest biomass from plot networks is the subject of some debate[15]. However, the contemporary increase in tropical forest biomass is consistent with the large and increasing carbon sink on Earth's land surface derived from the mass-balance implications of fossil-fuel CO_2 emissions and atmospheric CO_2 measurements, along with the global role of woody tissue as the location of a large fraction of the terrestrial carbon sink[6].

Forest biomass carbon stocks in Asia and Africa are projected to be greater in year 2100 than at the present day, in all simulations. This is also true for the Americas/Amazon, except for the HadCM3 climate model. There is however a decreasing ability to sequester carbon in biomass; many pathways have a C_v peak towards the end of the twenty-first century. Figure 2 grey columns are commitment simulations where climate forcing (here, predicted for 2100) is maintained at that level for a sufficient period that terrestrial ecosystems fall in equilibrium with that amount of climate change. Generally this increases the spread of simulations, where those with higher vegetation carbon at the end of the twenty-first century show an even higher uptake for the committed period, and simulations peaking earlier in the century show a further reduction. Particularly large differences between the final year of the transient simulations and committed values of C_v are, for Americas: major biomass loss for HadCM3 (confirming the analysis of ref. 16); and the MPI ECHAM 5 model predicts less C_v than that estimated in pre-industrial times.

We perform sensitivity simulations where only single patterns of meteorological change are added to the CRU climatology. This aids understanding of the mechanisms responsible for the changes in C_v. Figure 3 shows these changes, years 1860–2100, for the Americas/Amazon region, and decomposes them into the individual effects of temperature, rainfall and atmospheric $[CO_2]$. Predictions are most sensitive to changes in temperature
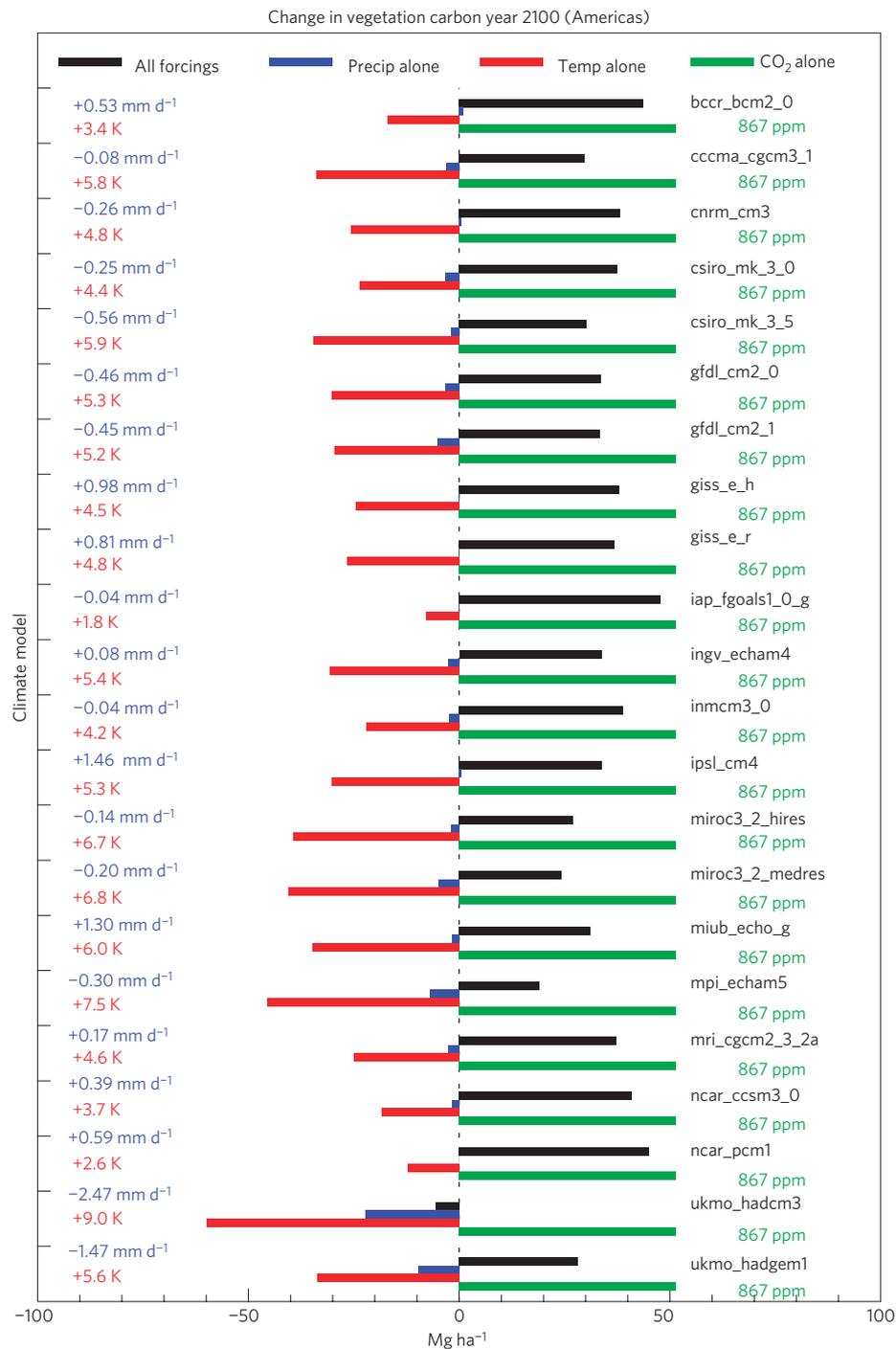
Figure 3 | Sensitivity of changes in biomass of Americas to different climate model drivers. Plot of changes to C_v for year 2100 minus 1860, for each climate model emulated. Included are sensitivity simulations for temperature change alone, rainfall change alone, CO_2 change alone, and for comparison against these, for all forcings. Also presented, as numbers on the plot, are the average yearly changes across the Amazon in the climatology associated with each sensitivity simulation.

and atmospheric [CO_2], with a lower sensitivity to precipitation alteration (Supplementary Fig. S4 shows the small sensitivity to other drivers such as wind speed change). Future changes in temperature would lead to reduced C_v, if not for our modelled positive response of vegetation to elevated atmospheric carbon dioxide[3,17]. Hence, the likelihood of die-back could be altered depending on the future balance of raised greenhouse-gas concentrations, with non-CO_2 gases such as methane having no fertilization effect[18]. Identical plots (Supplementary Figs S2 and S3) for African

and Asian forests show again a balance predominantly between the effects of CO_2 fertilization and increased temperature, although there the temperature-alone changes are generally smaller in magnitude.

To place our analysis in the broader context of uncertainty in ecosystem description, we extract changes in biomass for the same three regions from ecological parameter perturbation experiments (PPE) that use the HadCM3C climate model[2], and from a dynamic global vegetation model (DGVM) inter-comparison study[1]. The
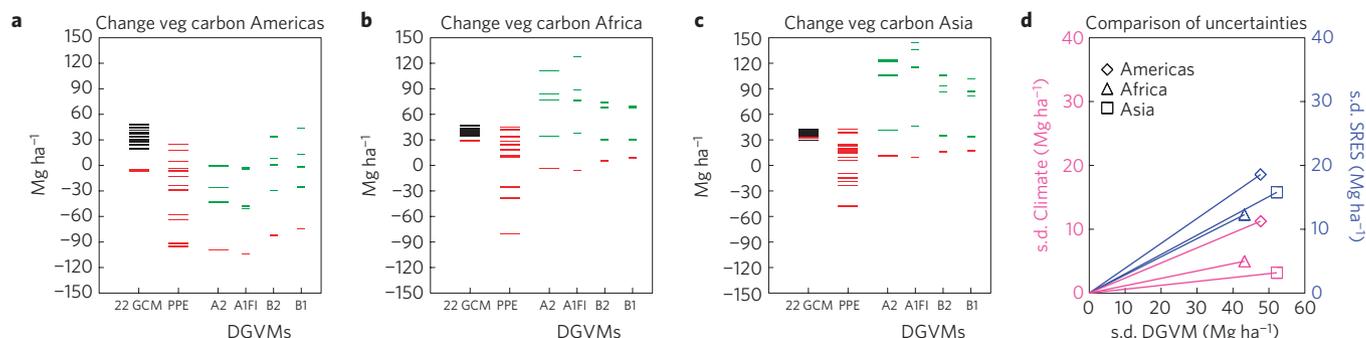
Figure 4 | Contributions of model uncertainties. a–c, For the three regions, spread of changes in C_v, 2100 value minus 1860. The 22-GCM label is the transient simulations presented in Fig. 2, all black except with the HadCM3 climate model in red. Similar calculations for the PPE with HadCM3C (all red) and the HadCM3-forced DGVM intercomparison simulations (DGVMs; SRES scenarios as marked and all green except MOSES–TRIFFID red). PPE and MOSES–TRIFFID for DGVMs are fixed-Q_{10} maintenance respiration. **d**, For all three regions, estimates of s.d. values between climate models (magenta axis) and between SRES scenarios (blue axis) are plotted against s.d. values between the DGVMs.

latter includes inter-DGVM structural differences (and different CO_2-fertilization responses), also with climate-change drivers from HadCM3. Figure 4a–c presents these changes in C_v by 2100, compared with 1860, for our 22-GCM simulations (values could be inferred from Fig. 3; red bars are the HadCM3 model), then for PPE (forced with SRES A1B emissions, a scenario with strong similarities to SRES A2), and finally the DGVM inter-comparison study (five models, four SRES scenarios). The red bars in the DGVM values are for MOSES–TRIFFID, and these and the PPE simulations are for fixed-Q_{10} representation of maintenance respiration. This corresponds to lower year 2100 biomass contents, particularly for the Americas and HadCM3 driving model (Supplementary Fig. S5). Figure 4d shows vectors of uncertainty, comparing estimates of standard deviation (s.d.) in climate uncertainty and s.d. between SRES scenarios, both plotted against s.d. values due to DGVM differences. The DGVM response uncertainty dominates over variation between climate models and emission scenarios. Limited but illustrative overall statistics are based on combining these three s.d. values to estimate uncertainty, and a calculated mean of the DGVM/SRES simulations offset by the HadCM3 difference from the 22-GCM mean (from the first columns, Fig. 4a–c). Fitting a normal distribution, this returns across ecosystem model, scenario and climate model probabilities of biomass decrease by year 2100 of 40% for the Americas, and 7% for both Africa and Asia (Methods). An alternative statistic, SRES A2 alone, is to adopt the MOSES–TRIFFID simulation from our 22-GCM simulations (red bar, first columns of Fig. 4a–c) to replace that from the DGVM intercomparison (red bar, A2 DGVM column). Then the probabilities of biomass decrease by year 2100, after similar mean offset, become 16% for the Americas, 2% for Africa and 4% for Asia (Methods).

With the largest uncertainty being land surface description, then the timing and magnitude of any projections of tropi-cal forest cover will depend strongly on modelled response to higher temperatures, elevated [CO_2] concentrations and changes in precipitation regimes. Figure 4 complements other studies; for instance, the LPJ (Lund Potsdam Jena) ecosystem model predictions of Amazon die-back forced across climate models[4] include one configuration showing less resilience[19]. Reducing this ecological uncertainty requires many parameters to be re-fined and possibly new process depiction. Free-air CO_2 enrich-ment experiments (FACE) artificially maintain carbon dioxide at raised concentrations[20], and do demonstrate a CO_2-fertilization effect in temperate post-disturbance forests. However, at present

there are no such experiments in tropical forests. Studies[20] indicate that productivity may eventually become constrained by nutrient limitation, which could therefore increase vulnerability to climate change. For tropical ecosystems there is good evidence that soil phosphorus is the dominant limiting nutrient (more limiting than nitrogen)[21,22]. However, the magnitude of this constraint remains uncertain, with several mechanisms potentially allowing extra phosphorus to be taken up from the soil to support at least some increased rates of plant growth at higher [CO_2] (ref. 23).

Uncertainty exists in physiological response to elevated temperatures[3,17]. We describe vegetation maintenance respiration as following a roughly bell-shaped response to temperature (or a declining-Q_{10}; ref. 24), and peaking around 32 °C. Other versions of MOSES–TRIFFID have assumed an exponential fixed-Q_{10} increase with increasing temperatures and existing Amazon studies[3,25] show that this process representation has a large effect on future modelled carbon stocks. Supplementary Fig. S5 plots C_v for both and reiterates that future values are significantly lower for a fixed-Q_{10} increase. Our peak temperature of 32 °C is lower than some reports[24], and as such Supplementary Fig. S5 can be regarded as providing upper and lower bounds on biomass implications due to this uncertainty in respiration response. There is also increasing evidence that the long-term temperature response of respiration is dynamic, capable of thermal acclimation[26]. Generally, acclimation, again not yet included in any major land surface model, is believed to mitigate the rate of increase in respiration rates in the event of a transition to warmer temperatures. There are suggestions that photosynthesis can also acclimate to rising temperatures[27], although the extent to which this might occur in tropical forest species remains unknown. Although our sensitivity simulations suggest that elevated temperature could be more detrimental to forest biomass than any climate-model-predicted decrease in rainfall, recent field data suggest that tropical forest function may be impeded in unusually dry years owing to strong seasonal moisture deficits. Using a basin-wide plot network in Amazonia[12], an increased mortality was observed in areas affected by the year 2005 Amazon drought[28]. More details expanding on present uncertainties are given in the Supplementary Information.

We find the possibility of climate-induced (that is, not di-rect deforestation) damage to tropical rainforests in the pe-riod to year 2100, even under the SRES A2 business-as-usual emissions scenario, might be lower than some earlier studies suggest. For instance, our MOSES–TRIFFID model configura-tion predicts undisturbed tropical forests as always sequester-ing carbon to mid twenty-first century, and possibly beyond

for most climate models. Such a result has implications for the United Nation's Reducing Emissions from Deforestation and Degradation+ scheme, which has previously been questioned owing to concerns over the resilience of the carbon stored in tropical forests. Physiological processes, rather than differences amongst climate projections, dominate uncertainties in the amount of future carbon accumulation in undisturbed tropical forests, but we anticipate that emerging data and ecological understanding will reduce this substantially in the next generation of land surface models.

Methods

Our land surface model for assessing climate uncertainty effects alone is the Met Office Surface Exchange Scheme 2.2 (MOSES) coupled to the DGVM top-down representation of interactive foliage and flora including dynamics (TRIFFID); now part of the JULES model[29]. MOSES–TRIFFID has been used in previous Amazon-dieback investigations[3,5,25], but there are two differences. First, soil parameterizations include new reported values. Second, dark respiration has the same temperature response as the maximum rate of carboxylation, $V_{c,max}$. This is the R_d term of equation (13) in ref. 29 and its influence on the canopy-level plant respiration fluxes is in equations (39)–(42) of ref. 29. For broad-leaved trees, we used the JULES formulation for $V_{c,max}$, peaking at leaf temperature around $32\,°C$. Many earlier studies set leaf respiration monotonically increasing with temperature following an exponential Q_{10} function, where $Q_{10} = 2.0$. Respiration peaking in temperature is more appropriate because (in photosynthetic and non-photosynthetic organs) it is known to ultimately decline as temperatures increase[24]. Data on peak temperature of tropical tree leaf respiration are limited. Our relatively low peak value versus the $Q_{10} = 2.0$ formulation may provide bounds on this uncertainty.

MOSES–TRIFFID is forced by a common base climatology plus patterns of changing meteorological conditions fitted against the 22 CMIP3 climate models. We employ pattern-scaling to calculate change, where regional and seasonal changes are assumed linear in global warming[30]. An energy balance model calculates global warming amount, also fitted to the CMIP3 ensemble. Precipitation patterns however are normalized against the CRU data set. For geographical position, month and a unit of global warming, each climate model predicts a percentage change in rainfall compared with its estimate of pre-industrial rainfall values. We then calculate the anomaly pattern as that percentage change applied to the CRU climatology estimate of precipitation. This combined impacts system, IMOGEN (ref. 14), is forced with historical concentrations followed by a standard pathway in atmospheric CO_2 concentrations associated with the business-as-usual SRES A2 emissions scenario, reaching 867 ppm in 2100. For non-CO_2 greenhouse gases and aerosols, an extra radiative forcing change is prescribed to the energy balance model. The modelling system is operated with a disturbance fraction for each gridbox appropriate for the end of the past century. This is assumed invariant into the future, and hence we do not take into account any future potential direct deforestation.

Adding anomalies of change to the CRU data set removes model biases. We estimate the pre-industrial state as averaged monthly CRU values for 1960–1989, recognizing that these include anthropogenically induced climate change up to that date. We assumed this error to be smaller than errors through using much earlier years in the CRU climatology, owing to the presence of many more contributing tropical meteorological measurements. This discrepancy is certainly much smaller than the large biases removed from the climate models (Supplementary Fig. S1). For the Americas, all 22 climate models have rainfall predictions that are too low. These biases can be as large as predicted change in climate (compare with temperature and rainfall magnitudes, left side Fig. 3).

Biomass inventory data are from the RAINFOR network across South America[12] (measurements from 123 plots) and from the AfriTRON network across Africa[13] (79 plots). The geographical spread of measurements for South America is not as large as the Americas region depicted in Fig. 1. There are only a few plots in the Central Congo Basin for the African data set. These data sets are relatively sparse compared with the extent of tropical forest, but are the most geographically widespread measurements of tropical biomass available at present. To compare with model outputs, corrections were applied to include stems smaller than those measured in each plot (<100 mm diameter). We do not consider necromass (coarse woody debris). For South America, measurements used are 1980–2005; measurements following the 2005 drought indicate a reduced rate of sequestration[6,12] but it is unknown whether this is a short-term perturbation or the beginning of a lower rate of net carbon uptake. African measurements used are 1987–1997, the mean start and end census dates of the 79 plots. We normalize spatially averaged inventory numbers to equal mean C_v across the 22 simulations in years 1980 (South America) and 1987 (Africa). Yearly percentage changes in mean, and 97.5% and 2.5% confidence levels equal those measured, and these normalized changes are plotted in Fig. 1.

Variance of changes in C_v between DGVMs (square of s.d values in Fig. 4d) is the average of, for each SRES scenario, expected variance across the five models. Similarly, variance between SRES scenarios is calculated by averaging, for each DGVM, the variance across scenarios. Adding these two values to the extra variance across the 22-GCM simulations gives total variance. An overall mean is calculated across the 20 DGVM simulations (5 models, 4 scenarios). We account for the HadCM3 climate model being used only in the DGVM intercomparison study by offsetting the overall mean by the difference between the mean of the 22 climate simulations and the HadCM3 simulation (red bar versus mean value of the 22-GCM columns; Fig. 4a–c). These mean and variance values provide the first illustrative probabilities of biomass loss under an assumption of normal distribution. The second set of probabilities are similarly calculated, with our HadCM3-forced MOSES–TRIFFID simulation replacing that in the DGVM-study for SRES A2. Now the mean is calculated across the SRES A2 DGVM simulations, and offset as above. Variance is the sum of variance across SRES A2 DGVMs combined with that across the 22-GCM runs.

The Supplementary Information gives further discussions of the methods and ecological uncertainties.

References

1. Sitch, S. et al. Evaluation of the terrestrial carbon cycle, future plant geography and climate-carbon cycle feedbacks using five dynamic global vegetation models (DGVMs). Glob. Change Biol. **14,** 2015–2039 (2008).
2. Booth, B. B. B. et al. High sensitivity of future global warming to land carbon cycle processes. Environ. Res. Lett. **7,** 024002 (2012).
3. Galbraith, D. et al. Multiple mechanisms of Amazonian forest biomass losses in three dynamic global vegetation models under climate change. New Phytol. **187,** 647–665 (2010).
4. Rammig, A. et al. Estimating the risk of Amazonian forest dieback. New Phytol. **187,** 694–706 (2010).
5. Cox, P. M., Betts, R. A., Jones, C. D., Spall, S. A. & Totterdell, I. J. Acceleration of global warming due to carbon-cycle feedbacks in a coupled climate model. Nature **408,** 184–187 (2000).
6. Pan, Y. et al. A large and persistent carbon sink in the world's forests. Science **333,** 988–993 (2011).
7. Beer, C. et al. Terrestrial gross carbon dioxide uptake: Global distribution and covariation with climate. Science **329,** 834–838 (2010).
8. Gardner, T. A. et al. Prospects for tropical forest biodiversity in a human-modified world. Ecol. Lett. **12,** 561–582 (2009).
9. Malhi, Y. et al. Exploring the likelihood and mechanism of a climate-change-induced dieback of the Amazon rainforest. Proc. Natl Acad. Sci. USA **106,** 20610–20615 (2009).
10. Zelazowski, P., Malhi, Y., Huntingford, C., Sitch, S. & Fisher, J. B. Changes in the potential distribution of humid tropical forests on a warmer planet. Phil. Trans. R. Soc. A **369,** 137–160 (2011).
11. Gumpenberger, M. et al. Predicting pan-tropical climate change induced forest stock gains and losses-implications for REDD. Environ. Res. Lett. **5,** 014013 (2010).
12. Phillips, O. L. et al. Drought sensitivity of the Amazon rainforest. Science **323,** 1344–1347 (2009).
13. Lewis, S. L. et al. Increasing carbon storage in intact African tropical forests. Nature **457,** 1003-U1003 (2009).
14. Huntingford, C. et al. IMOGEN: An intermediate complexity model to evaluate terrestrial impacts of a changing climate. Geosci. Model Dev. **3,** 679–687 (2010).
15. Gloor, M. et al. Does the disturbance hypothesis explain the biomass increase in basin-wide Amazon forest plot data? Glob. Change Biol. **15,** 2418–2430 (2009).
16. Jones, C., Lowe, J., Liddicoat, S. & Betts, R. Committed terrestrial ecosystem changes due to climate change. Nature Geosci. **2,** 484–487 (2009).
17. Lloyd, J. & Farquhar, G. D. Effects of rising temperatures and [CO_2] on the physiology of tropical forest trees. Phil. Trans. R. Soc. B **363,** 1811–1817 (2008).
18. Huntingford, C. et al. Highly contrasting effects of different climate forcing agents on terrestrial ecosystem services. Phil. Trans. R. Soc. A **369,** 2026–2037 (2011).
19. Scholze, M., Knorr, W., Arnell, N. W. & Prentice, I. C. A climate-change risk analysis for world ecosystems. Proc. Natl Acad. Sci. USA **103,** 13116–13120 (2006).
20. Norby, R. J., Warren, J. M., Iversen, C. M., Medlyn, B. E. & McMurtrie, R. E. CO(2) enhancement of forest productivity constrained by limited nitrogen availability. Proc. Natl Acad. Sci. USA **107,** 19368–19373 (2010).
21. Quesada, C. A. et al. Basin-wide variations in Amazon forest structure and function are mediated by both soils and climate. Biogeosciences **9,** 2203–2246 (2012).

22. Mercado, L. M. *et al.* Variations in Amazon forest productivity correlated with foliar nutrients and modelled rates of photosynthetic carbon supply. *Phil. Trans. R. Soc. B* **366,** 3316–3329 (2011).
23. Lloyd, J. in *Global Biogeochemical Cycles in the Climate System* (eds Schulze, E. D. *et al.*) (Academic, 2001).
24. Tjoelker, M. G., Oleksyn, J. & Reich, P. B. Modelling respiration of vegetation: Evidence for a general temperature-dependent Q(10). *Glob. Change Biol.* **7,** 223–230 (2001).
25. Huntingford, C. *et al.* Using a GCM analogue model to investigate the potential for Amazonian forest dieback. *Theor. Appl. Climatol.* **78,** 177–185 (2004).
26. Atkin, O. K. & Tjoelker, M. G. Thermal acclimation and the dynamic response of plant respiration to temperature. *Trends Plant Sci.* **8,** 343–351 (2003).
27. Medlyn, B. E., Loustau, D. & Delzon, S. Temperature response of parameters of a biochemically based model of photosynthesis. I. Seasonal changes in mature maritime pine (*Pinus pinaster* Ait.). *Plant Cell Environ.* **25,** 1155–1165 (2002).
28. Marengo, J. A. *et al.* The drought of Amazonia in 2005. *J. Clim.* **21,** 495–516 (2008).
29. Clark, D. B. *et al.* The joint UK land environment simulator (JULES), model description—part 2: Carbon fluxes and vegetation dynamics. *Geosci. Model Dev.* **4,** 701–722 (2011).
30. Huntingford, C. & Cox, P. M. An analogue model to derive additional climate change scenarios from existing GCM simulations. *Clim. Dynam.* **16,** 575–586 (2000).

Author contributions

C.H. designed the overall paper; P.Z. built the climate patterns; D.G. and L.M.M. created the sensitivity framework; S.S., R.F., C.D.J., R.B., Y.M., P.G. and P.P.H. provided climate-change and ecosystem expertise, and aided with the context placing of this analysis in terms of existing literature on tropical-forest/climate-change interactions; M.L. and B.B.B.B. helped with IMOGEN development; A.P.W., D.H., O.K.A., J.L., E.G., J.Z-C. and P.M. built the discussion of remaining questions in physiological responses; G.K. provided information on REDD, S.L.L. and O.L.P. provided the Amazon and Africa inventory data and C.N. and J.M. updated on Brazilian research. B.B.B.B. provided diagnostics from the PPE, S.S. provided diagnostics from the DGVM-intercomparison study and P.M.C. aided with the uncertainty analysis and overall conclusions. All authors contributed to the writing of the manuscript.

Additional information

Supplementary information is available in the online version of the paper. Reprints and permissions information is available online at www.nature.com/reprints. Correspondence and requests for materials should be addressed to C.H.

Competing financial interests

The authors declare no competing financial interests.